

Research Article

Design of Compact Trapezoidal Bow-Tie Chipless RFID Tag

Lei Xu and Kama Huang

School of Electronics and Information Engineering, Sichuan University, Chengdu 610064, China

Correspondence should be addressed to Kama Huang; huangkamasu@21cn.com

Received 23 July 2014; Accepted 17 October 2014

Academic Editor: Antonio Faraone

Copyright © 2015 L. Xu and K. Huang. This is an open access article distributed under the Creative Commons Attribution License, which permits unrestricted use, distribution, and reproduction in any medium, provided the original work is properly cited.

This paper presents a novel compact design of a low cost fully printable slot-loaded bowtie chipless RFID tag. The tag consists of two trapezoidal metallic patches loaded with multiple slot resonators. Slots with similar size or adjacent frequencies are loaded alternately on two bow-tie patches to double the number of data bits within the UWB frequency band without increasing the mutual coupling between slots. A coding capacity of 12 bits is obtained with 12 slots within a reasonable size of 35 mm × 33 mm. RCS of the tag has been given by simulation. Measurements have been done using a bistatic radar configuration in the frequency domain and transmission coefficient is measured. The agreement between the simulation and measurement validates this new concept of design. This tag has high data capacity and low cost and can be directly printed on product such as personal ID, credit cards, paper, and textile because it needs only one conductive layer.

1. Introduction

Radio frequency identification (RFID) is an automatic identification technology that uses EM waves to extract encoded data from remote tags [1, 2]. The RFID tag has some advantages over the current mainstream optical barcode [3], such as longer reading range, non-line-of-sight reading, and automated identification and tracking, and consequently has the potential to replace the barcode [4]. However, conventional RFID tag contains silicon chip and antenna and thus has higher cost, making it difficult to compete with the low cost barcode technology. Therefore, research effort has been focused on another promising candidate, that is, chipless RFID tag, which would not require any chip nor communication protocol and can be used like barcode. The concept of RF barcode was firstly introduced by Jalaly and Robertson [5], and then it was developed worldwide [6]. A chipless tag acts as a transmitting antenna, a receiving antenna, and a filter simultaneously. However, the tag without chip is inflexible to encode high density data on it. Increasing data capacity, enhancing robustness, and reducing size and cost are the current challenges of designing chipless tag.

At present, there are various designs of chipless RFID tags, which can be classified according to their encoding method. Some tags are encoded in the time domain [5, 7, 8], while

others are encoded in frequency domain [9–12]. Frequency domain-based tags have higher data density and are more easily to be miniaturized than time domain-based tags. A 3-bit notched elliptical dipole tag has been presented in [13] and the singularity based encoding is firstly applied in RFID tag, but the coding capacity of this tag is too low to be used outside the lab. Hybrid coding technique for chipless tag has been presented in [14] with coding capacity up to 23 bits, but the required frequency resolution cannot be easily implemented for data encoding. A chipless tag consisting of multiple stopband spiral resonators and two cross polarized UWB antennas has been presented in [15]. A 16-bit fully printable slot-loaded dual-polarized chipless RFID tag has been presented in [16] with improving coding efficiency with the aid of a pair of dual-polarized antennas.

In this paper, a bow-tie chipless RFID tag is presented. It consists of two symmetrical trapezoidal metallic patches loaded with 12 pairs of slot resonators corresponding to 12-bit data. High data capacity is achieved by the tapering length of slot resonators loaded on a patch. This compact tag has a reasonable physical size of 35 mm × 33 mm and it operates within the UWB frequency band. Higher data capacity can be obtained by adjusting the width of the slot and the metal strip. Compared with other designs, the proposed design is more compact and easier to be implemented.

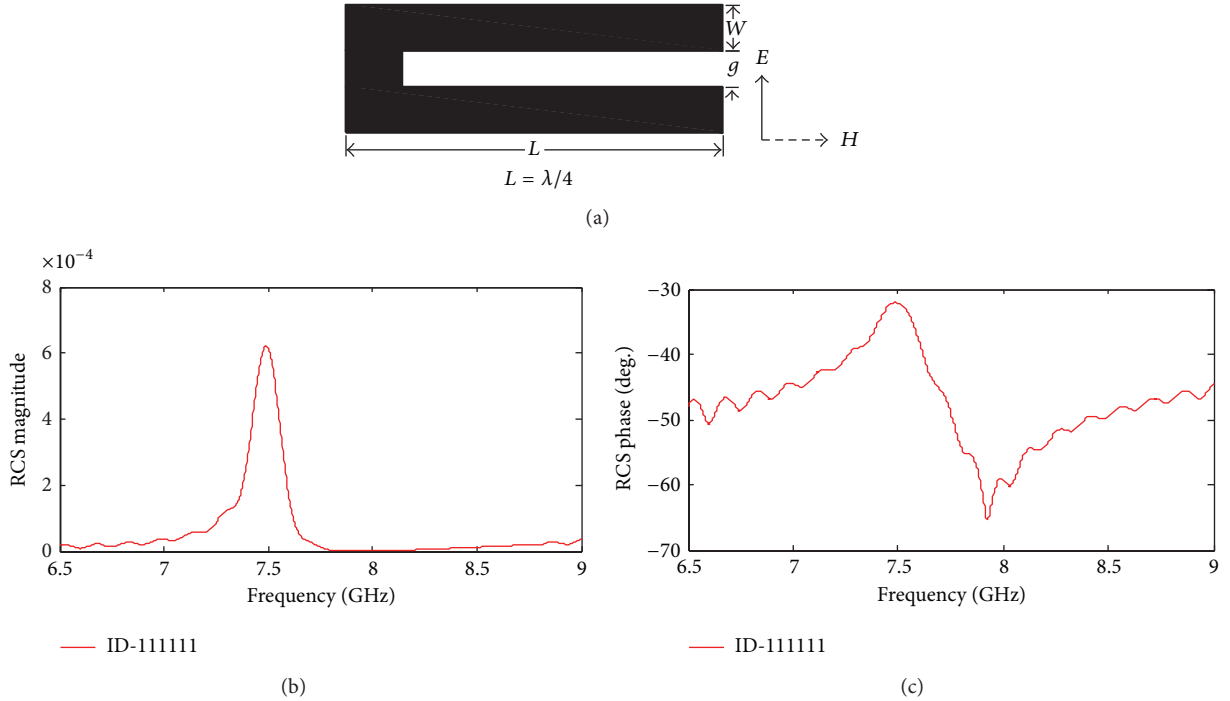


FIGURE 1: (a) Basic resonance element using slot resonator, the dimensions are $L = 8.5$ mm, $W = 1.5$ mm, and $g = 0.5$ mm. (b) Magnitude versus frequency response of slot resonator. (c) Phase versus frequency response of slot resonator.

The rest of the paper is organized as follows: Section 2 presents operating principle of the proposed chipless RFID tag. Section 3 presents the design and simulation of the tag. Section 4 presents measurement results compared to simulations followed by conclusion in Section 5.

2. Basic Principle

2.1. Principle of the Loaded Resonator. A metallic patch loaded with several slot resonators can create a radar cross section (RCS) with some sharp notches or peaks at specific frequencies in the backscattering signal, and these notches or peaks can be used to encode data within a frequency band.

A single slot resonator used in the proposed tag, shown in Figure 1(a), is a planar strip having a length L and a gap width g . One side of the slot is shorted; the other side is open. When the guided quarter wavelength matches the physical length L , a quarter wavelength standing wave modes is excited by an incident vertical polarized electromagnetic wave perpendicular to this asymmetrical slot, and a minimum surface current is induced on the open side of the slot resonator and a maximum surface current is induced on the short side. The magnitude-frequency response and phase-frequency response are shown in Figures 1(b) and 1(c), respectively. Furthermore, the capacitive effect between two arms of the slot resonator increases the quality of the resonator. A narrow band resonance cannot be excited on this tag by a horizontal polarized wave. In addition to a resonance, there is an antiresonance which comes from the spatial cancellation of the fields. The antiresonance relies

on the polarization and incident angle of the exciting wave [17]. This resonator has intrinsically a resonant peak and an antiresonant dip in its spectrum, which can be used to encode data.

The resonant frequency of the slot resonator can be estimated using [18]

$$f_r = \frac{c}{2L} \sqrt{\frac{2}{1 + \epsilon_r}}. \quad (1)$$

Here, c is the speed of light and ϵ_r is the relative permittivity of the substrate. Besides, the gap width g also has a slight influence on the resonance frequency. Considering these two factors, the resonant frequency of the slot resonator depends on the length $L + g/2$. Quality factor of the slot is proportional to the ratio L/g . Therefore, the resonant frequency and quality factor can be easily adjusted by the slot length L and gap width g , respectively. One or more slots can be loaded on a metallic patch, and one or more slots of the resonator can be shorted and the corresponding frequencies are thus nulled, and a data bit 0 or 1 can be encoded according to the presence or absence of a peak or dip in the spectrum. The encoding rule used in this paper is very simple: the presence or absence of the dip presents data bit 1 or 0, respectively.

2.2. Operating Principle of the Proposed Chipless RFID Tag. Figure 2 shows the operating principle of the proposed RFID tag. When the chipless RFID tag is impinged by a vertically polarized EM wave from the transmitter antenna, a unique frequency signature is excited, and the receiver antenna receives the encoded backscattered signal. The RFID

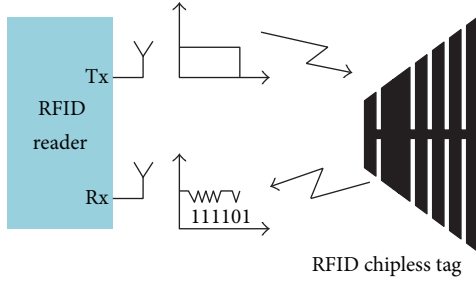


FIGURE 2: Principle of operation.

reader or measurement device records and extracts this unique frequency signature, and the chipless RFID tag is thus identified.

3. Design and Simulation of the Chipless Tag

The configuration of the proposed trapezoidal chipless RFID tag I and tag II is depicted in Figure 3.

A trapezoidal metallic patch with bottom width W_b , top width W_t , and height H acts as a carrier of slot resonators. Six pairs of quarter-wavelength open-ended slot resonators with different length L_i ($i = 1, 2, 3, 4, 5, 6$) are loaded on the trapezoidal metallic patch. The 6 pairs of slot resonators with different physical dimensions create 6 peaks and 6 dips in spectrum corresponding to 6 resonant frequencies. The six physical slots with different length from the longest to the shortest create six quarter-wavelength resonances, and the corresponding frequencies, from the lowest to the highest, are 4.1 GHz, 4.8 GHz, 5.8 GHz, 6.5 GHz, 8.3 GHz, and 10.3 GHz. In order to facilitate the fabrication, the width s of the slot of these resonators keeps the same size of 0.5 mm. Simulation results are shown in Figure 4.

The coding principle used for this tag is very simple: each resonant frequency has a peak and dip in spectrum, and the dip is chosen to encode 1 data bit. Six dips are seen in the magnitude response for six 1's of the tag with ID "111111," while five dips are seen for five 1's as opposed to no dip for the 0 in the magnitude response for the tag with ID "111101." Six phase jumps are seen in the phase response for the tag with ID "111111," but no phase jumps for the 0 for the tag with ID "111101." The phase response can double check the magnitude response.

Although higher data capacity can be obtained by loading more slot resonators, there exists mutual coupling of considerable strength between adjacent resonators when the slot resonators are located close to each other. Therefore, to double the data bits without increasing mutual coupling between adjacent slots, two identical metallic patches are placed symmetrically on the substrate. Six pairs of slot resonators on the right patch remain unchanged and the length of the six pairs of slot resonators is L_i ($i = 1, 2, 3, 4, 5, 6$), while six pairs of slot resonators on the left patch are integrally shifted 1 mm to the top side of the trapezoid patch, and the length of these six pairs of slot resonators is L_i ($i = 7, 8, 9, 10, 11, 12$). Figure 5 shows the proposed bow-tie chipless tag III and

TABLE I: Fabricated tag dimension in mm.

Tag	Encoded data	L	W	H	H_0	H_1	W_0	W_t	W_b	s
I	111111	33	18							
II	111101			14	2	1.5	1	6	28	0.5
III	111111111111	35	33							
IV	011111111110									

tag IV. The twelve physical slots with different length from the longest to the shortest create twelve quarter-wavelength resonances, and the corresponding frequencies, from the lowest to the highest, are shown in Figure 6.

One bit data correspond to one frequency. Therefore, the tag can present 12-bit data and has a unique frequency signature. To configure the tag, each slot resonator can be shorted or not depending on the encoded data. The presence and absence of a given frequency band present data bits 1 and 0, respectively.

When all of these slots keep unfilled, the 12-bit tag represents ID1: 111111111111, as shown in Figure 5(a). When some of these slot are shorted, the relevant frequencies will be nulled; for example, when the longest slot on the left side, that is, L_1 , and the shortest slot on the right side, that is, L_{12} , are filled, this tag represents ID2: 011111111110, as shown in Figure 5(b). In our case, there is no ground plane, and the size of this structure is nearly 35 mm \times 33 mm.

4. Fabrication and Measurements

For the measurement, four tags with different ID have been fabricated. The fabricated tags are illustrated in Figure 7 and the dimensions of the tags are shown in Table I. The tags are implemented on a FR-4 substrate with a permittivity of 4.4, a loss tangent of 0.023, and a thickness of 0.5 mm. FR-4 is a versatile and usually a low cost substrate and the fabrication process is based on copper etching.

The measurement may be done in anechoic chamber or in real office environment with tables, walls, and various wireless devices. A bistatic radar system is used to detect data encoded in the chipless tag. The measurement system is composed of a vector network analyzer (VNA) AV3629D with an output power of 0 dBm in the entire measurement frequency band, connected to two identical UWB horn antennas having a minimum 10 dB of gain in the frequency band from 3.1 to 10.6 GHz. The two antennas are placed 10 cm away from each other and the tag under test is placed 15 cm from two antennas as shown in Figure 8. The transmitting antenna excites the resonators of the tag and the receiving antenna receives its EM signature as for a bistatic radar system.

The transmission coefficient S_{21} is measured and plotted against frequency in Figure 9. Due to fabrication error and measurement error, the measuring resonance frequencies are shifted slightly from the simulating resonance frequencies. Here, the frequency shift is within the ± 200 MHz band around the designed frequency. Therefore, the binary IDs still can be extracted from the four tags properly, and the

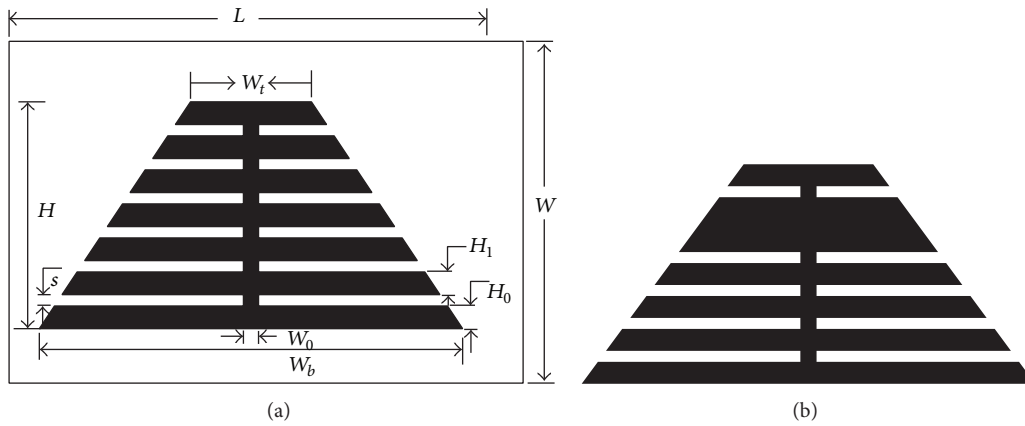


FIGURE 3: (a) Trapezoidal tag I with ID “111111” loaded with six pairs of slot resonators. (b) Trapezoidal tag II with ID “111101” loaded with five pairs of slot resonators.

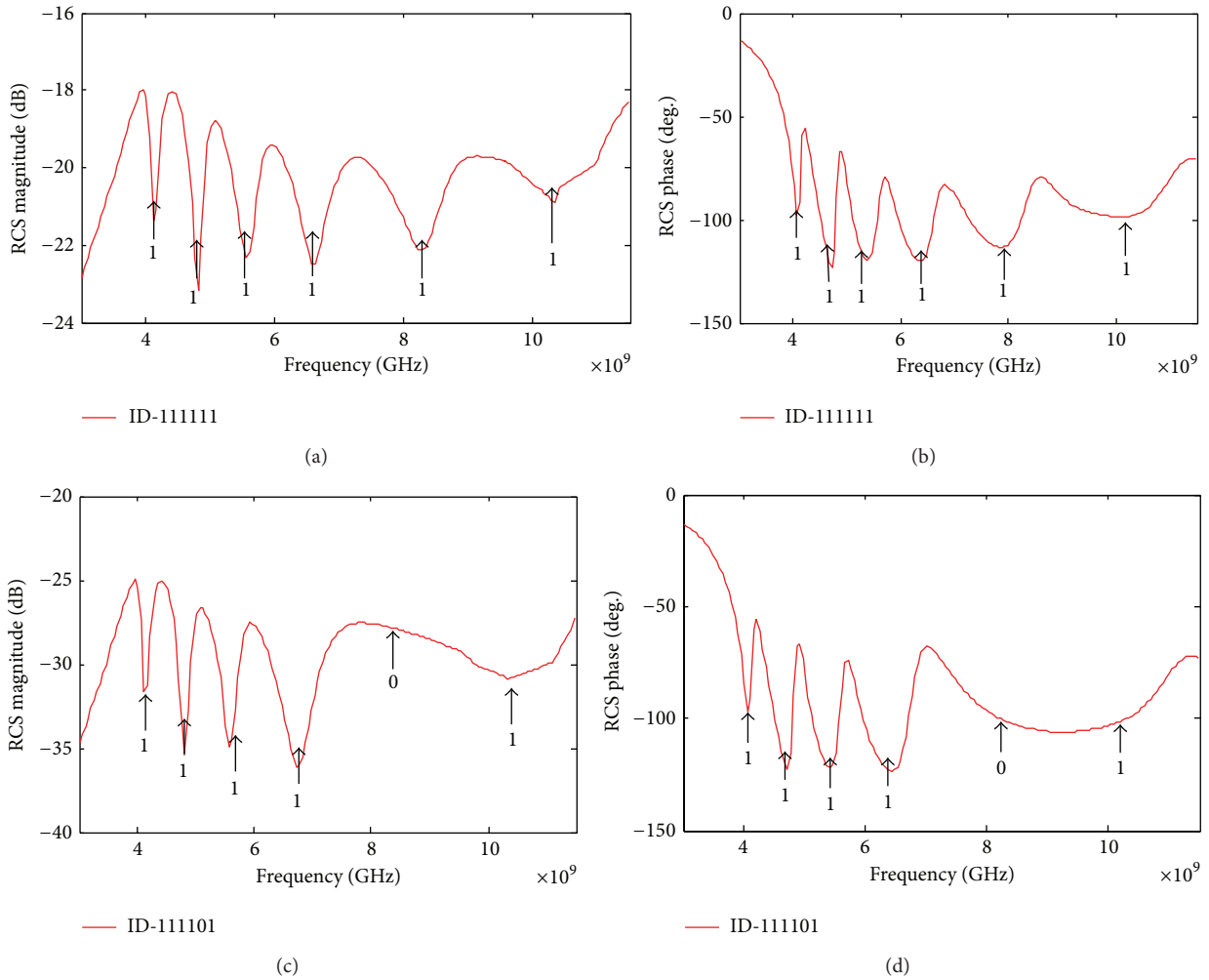


FIGURE 4: (a) RCS magnitude versus frequency simulation of tag I; (b) RCS phase versus frequency simulation of tag I; (c) RCS magnitude versus frequency simulation of tag II; (d) RCS phase versus frequency simulation of tag II.

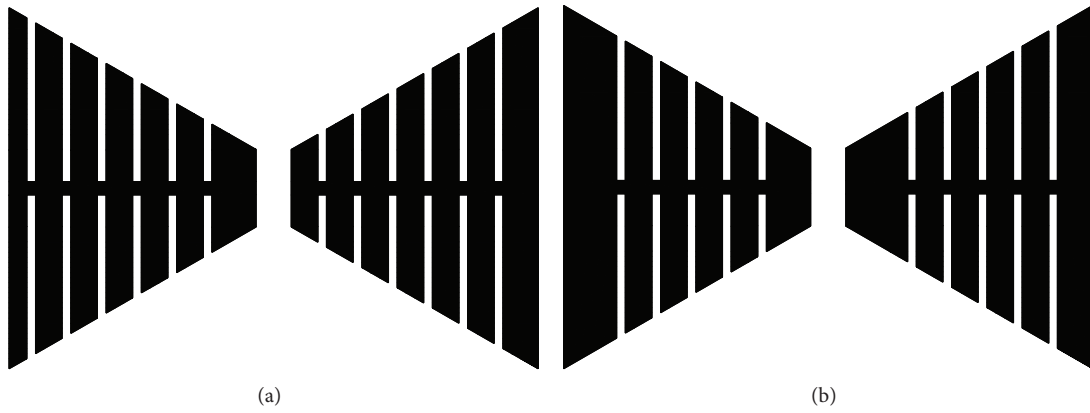


FIGURE 5: (a) The proposed bow-tie chipless RFID tag III with ID “111111111111”; (b) the proposed bow-tie chipless RFID tag IV with ID “011111111110.”

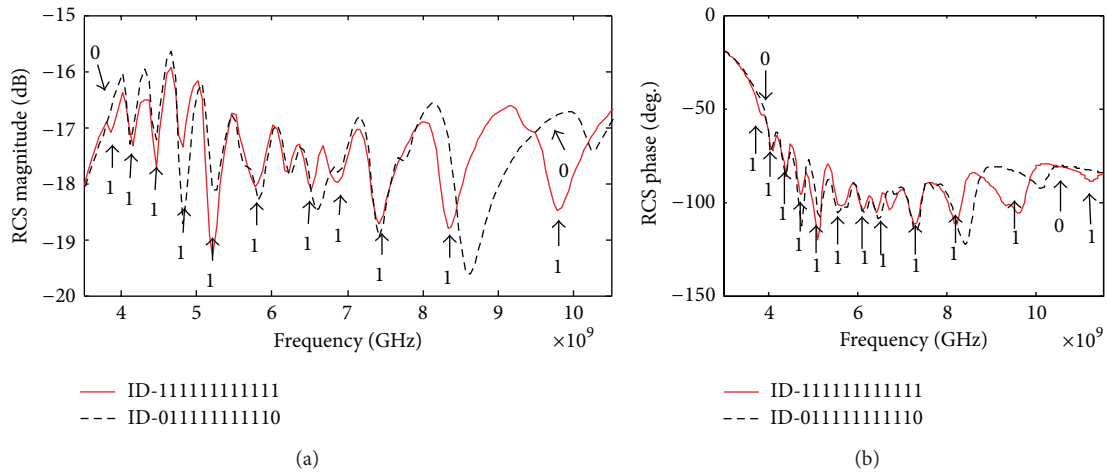


FIGURE 6: (a) Simulation of magnitude response for tag III and tag IV. (b) Simulation of phase response for tag III and tag IV.

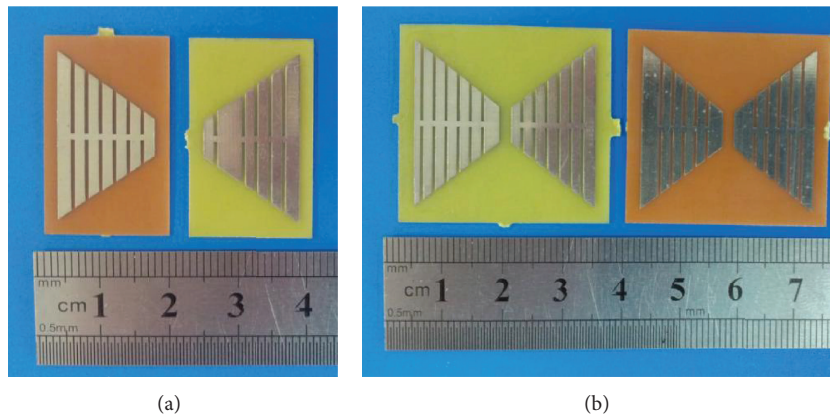


FIGURE 7: (a) Photograph of fabricated tag I and tag II. (b) Photograph of fabricated tag III and tag IV.

agreement between measurement results and simulation results validates this design of chipless RFID tag.

5. Conclusion

In this paper, a systematic method was presented for assigning and recovering multibit data in metallic patch.

A planar trapezoidal bow-tie RFID chipless tag was used as an ultrawideband structure, in which notch frequencies were introduced by placing slot resonators. In terms of data capacity, although 12-bit data are encoded in the proposed tag, higher capacity data can be designed for the same size. If the width of the slot s is set to 0.25 mm and the width of the metal strip H_1 is set to 0.75 mm, the data capacity

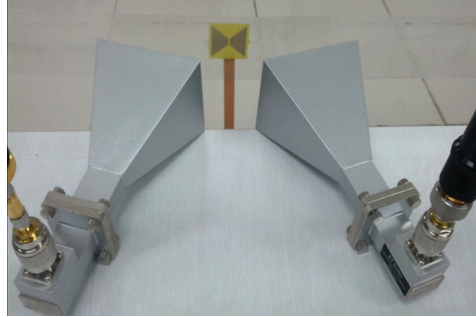


FIGURE 8: Measurement setup using bistatic configuration.

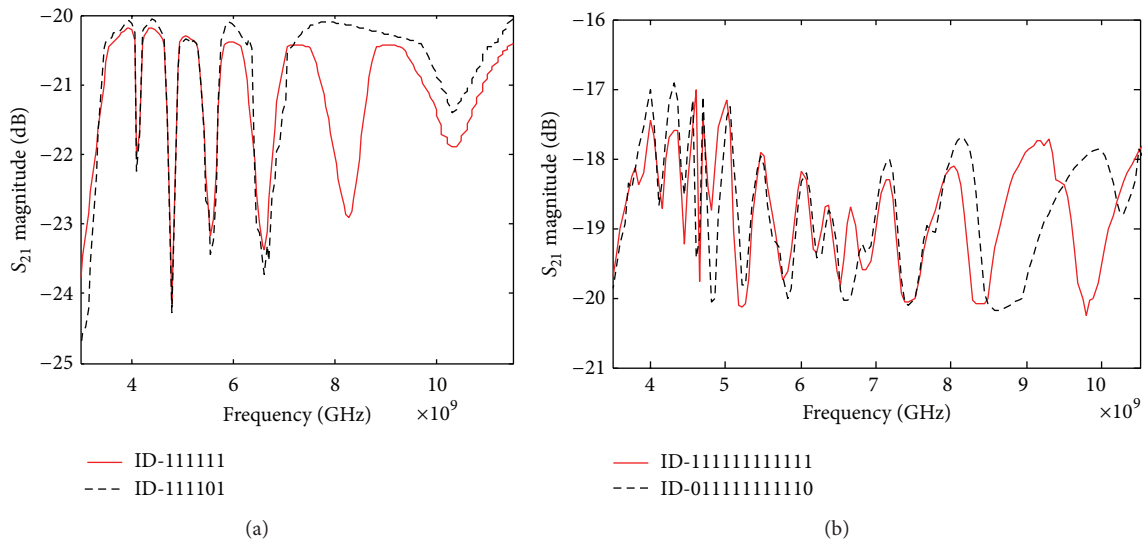


FIGURE 9: (a) The measurement results of tag I and tag II. (b) The measurement results of tag III and tag IV.

can be doubled, that is, up to be 24 bits within the same overall dimension. The simulation results revealed that these frequencies could be recovered in the RCS spectrum. The measurement results have validated the simulation results and thus validated this design. The low cost single sided compact chipless RFID tag can be printed directly on many items and can be used in many products such as paper and textile.

Conflict of Interests

The authors declare that there is no conflict of interests regarding the publication of this paper.

Acknowledgment

This project is supported by 973 Programs of China (National Basic Research Program of China, Project number 2013CB328705).

References

- [1] K. Finkenzeller, *RFID Handbook: Fundamentals and Applications in Contactless Smart Cards, Radio Frequency Identification and Near-Field Communication*, John Wiley & Sons, New York, NY, USA, 2010.
- [2] M. J. Uddin, A. N. Nordin, M. B. I. Reaz, and M. A. S. Bhuiyan, "A CMOS power splitter for 2,45 GHz ism band RFID reader in 0,18 μm CMOS technology," *Tehnicki Vjesnik*, vol. 20, no. 1, pp. 125–129, 2013.
- [3] D. Sun and D. Liu, "A novel RFID authentication protocol with ownership transfer," *Journal of Digital Information Management*, vol. 11, no. 6, pp. 476–481, 2013.
- [4] S. D. Hont, *The Cutting Edge of RFID Technology and Applications for Manufacturing and Distribution*, Texas Instrument TIRIS, Massachusetts, Ma, USA.
- [5] I. Jalaly and I. D. Robertson, "RF barcodes using multiple frequency bands," in *Proceedings of the IEEE MTT-S International Microwave Symposium Digest*, pp. 1–4, June 2005.
- [6] L. Zhong and L. Hou, "Nano-structured Si/C/N composite powder produced by radio frequency induction plasma and its microwave absorbing properties," *Journal of Engineering Science and Technology Review*, vol. 6, no. 2, pp. 160–163, 2013.
- [7] C. Mandel, M. Schüssler, M. Maasch, and R. Jakoby, "A novel passive phase modulator based on LH delay lines for chipless microwave RFID applications," in *Proceedings of the IEEE MTT-S International Microwave Workshop Series on Wireless Sensing, Local Positioning and RFID (IMWS '09)*, pp. 1–4, September 2009.

- [8] C. S. Hartmann, "A global SAW ID tag with large data capacity," in *Proceedings of the IEEE Ultrasonics Symposium*, vol. 1, pp. 65–69, October 2002.
- [9] R. Nair, E. Perret, and S. Tedjini, "Temporal multi-frequency encoding technique for chipless RFID applications," in *Proceedings of the IEEE MTT-S International Microwave Symposium (IMS '12)*, pp. 1–3, Montreal, Canada, June 2012.
- [10] S. Preradovic and N. Karmakar, "Design of fully printable planar chipless RFID transponder with 35-bit data capacity," in *Proceedings of the European Microwave Conference (EuMC '09)*, pp. 13–16, September 2009.
- [11] D. Girbau, J. Lorenzo, A. Lazaro, C. Ferrater, and R. Villarino, "Frequency-coded chipless RFID tag based on dual-band resonators," *IEEE Antennas and Wireless Propagation Letters*, vol. 11, pp. 126–128, 2012.
- [12] S. Preradovic and N. Kamakar, "Design of fully printable planar chipless RFID transponder with 35-bit data capacity," in *Proceedings of the 39th European Microwave Week*, Rome, Italy, September 2009.
- [13] A. T. Blischak and M. Manteghi, "Embedded singularity chipless RFID tags," *IEEE Transactions on Antennas and Propagation*, vol. 59, no. 11, pp. 3961–3968, 2011.
- [14] A. Vena, E. Perret, and S. Tedjini, "Chipless RFID tag using hybrid coding technique," *IEEE Transactions on Microwave Theory and Techniques*, vol. 59, no. 12, pp. 3356–3364, 2011.
- [15] S. Preradovic, S. M. Roy, and N. C. Karmakar, "RFID system based on fully printable chipless tag for paper-/plastic-item tagging," *IEEE Antennas and Propagation Magazine*, vol. 53, no. 5, pp. 15–32, 2011.
- [16] M. Aminul Islam and N. Karmakar, "Design of a 16-bit ultra-low cost fully printable slot-loaded dual-polarized chipless RFID tag," in *Proceedings of the Asia-Pacific Microwave Conference (APMC '11)*, pp. 1482–1485, December 2011.
- [17] A. Vena, E. Perret, and S. Tedjini, "A fully printable Chipless RFID tag with detuning correction technique," *IEEE Microwave and Wireless Components Letters*, vol. 22, no. 4, pp. 209–211, 2012.
- [18] T. Dissanayake and K. P. Esselle, "Prediction of the notch frequency of slot loaded printed UWB antennas," *IEEE Transactions on Antennas and Propagation*, vol. 55, no. 11, pp. 3320–3325, 2007.



Hindawi

Submit your manuscripts at
<http://www.hindawi.com>

